

# Surgical Structured Light for 3D Minimally Invasive Surgical Imaging

Austin Reiter, Alexandros Sigaras, Dennis Fowler and Peter K. Allen

**Abstract**—Surgeons perform minimally invasive surgery using an image delivered by a laparoscope and a camera system that provides a high definition 2D image, but this leaves the surgeon without 3D depth perception. The lack of depth perception can slow the surgeon, increase the risk of misidentifying structures, and/or inadvertently cause unwanted injury to tissues surrounding the surgical site. To address the lack of depth perception, we propose a Surgical Structured Light (SSL) system that includes a 3D sensor capable of measuring and modeling the surgical site during a procedure. The 3D information provided by this system can enable the surgeon to: 1) improve the navigation of tools based on precise localization of instruments in relation to structures in the surgical site, 2) allow 3D visualizations side-by-side with a standard 2D color image, and 3) precisely measure sizes of structures (e.g., tumors) and distances between structures with simple mouse clicks. We demonstrate the accuracy of our SSL system using ex-vivo data on both a cylinder calibration object as well as various plastic organs.

## I. INTRODUCTION

Minimally Invasive Surgery (MIS) in the abdomen and chest yields significantly better results than traditional open surgery in that patients have fewer complications, recover in less time, have much better cosmetic results, and the treatment of the underlying condition is at least as good, if not better, than open surgery [1]. Since the techniques of MIS were developed in the late 1980s and early 1990s, millions of patients have received the benefits of MIS. However, millions of other patients have not received the benefits of MIS because the limitations of currently available technology prevent many surgeons from completing complex operations using MIS techniques.

Traditionally, surgeons made an incision large enough to both visualize the surgical site and perform the surgery. In the late 1980s, a small digital camera coupled with a rod lens rigid endoscope enabled surgeons to visualize the surgical site through a small incision that was only large enough to accommodate the scope. That imaging technology (called laparoscopy) is still used in a vast majority of MIS cases. Although it currently provides a crisp, high definition image of the surgical site, laparoscopy delivers a 2-dimensional (2D) image of a 3-dimensional (3D) surgical site. The surgeon is unable to perceive depth, and for this reason, the overall use of MIS for complex operations remains limited. Additionally, the angle from which the surgical site is viewed is still severely limited by the location on the body wall of

A. Reiter, A. Sigaras, and P. K. Allen are with the Dept. of Computer Science, D. Fowler is with the Dept. of Surgery, Columbia University, New York, NY 10027, USA areiter@cs.columbia.edu, as4161@columbia.edu, dlf91@columbia.edu, allen@cs.columbia.edu,

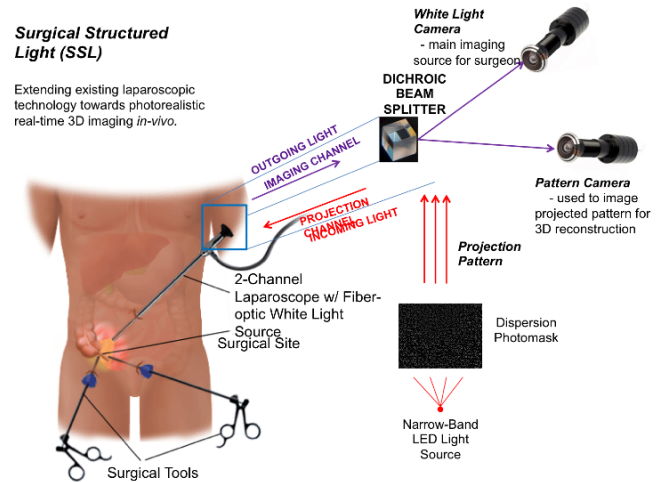


Fig. 1. A diagram of the various components of our SSL system. A narrow-band LED light projector coupled with a photomask projects a known pattern of light through a standard laparoscope (Projection Channel) into the surgical field. A second standard laparoscope (Imaging Channel) relays all of the light in the scene through a dichroic beam splitter, which feeds only the LED pattern light to one camera (Pattern Camera) and all other light, minus the pattern, to a second camera (White Light Camera). Algorithms use this optical setup to reconstruct photorealistic colored 3D reconstructions for use during MIS.

the incision through which the scope passes, and this further limits the visualization options. Both of these limitations contribute to misperception of structures in the surgical field, a situation that can result in costly injuries, both for the patient and for the healthcare system. These limitations of laparoscopic imaging slow the surgeon, lengthen the learning curve, and, in some complex cases, prevent the surgeon from completing the operation without making a large incision.

The work in this paper presents a new technology which is capable of providing surgeons with this missing 3D information using modern computational capabilities along with currently available imaging technologies. Our system, called Surgical Structured Light (SSL), provides: 1) 3D reconstructions of the surgery site, 2) unique, novel views not previously available using endoscopic imaging, and 3) 3D metrology. Using work described in this paper, the surgeon can manipulate the displayed 3D reconstruction to view the surgical site from multiple angles intra-operatively. With this technology, s/he can visualize the relationship between instruments and various structures within the surgical field, precisely measure the distance between structures in the surgical field, or potentially register the intra-operative images with pre-operative images (CT, MRI, or Ultrasound).

Stereo 3D imaging has been used to reconstruct soft tissue

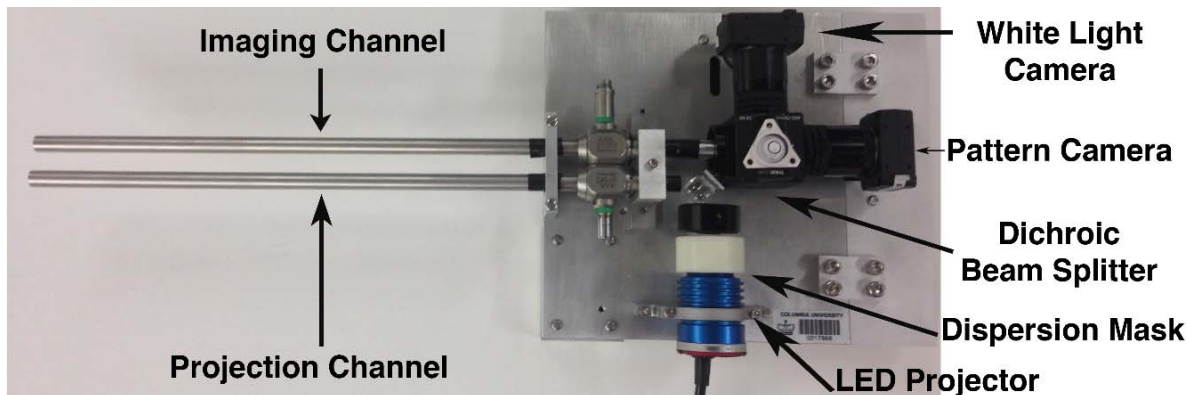


Fig. 2. An image of our prototype of the Surgical Structured Light (SSL) system. We use two standard, off-the-shelf, side-by-side 10mm laparoscopes for the projection and imaging channels. A narrow-band blue LED projector coupled with a photomask projects the pattern of light into the scene while the dichroic beam splitter relays the blue light to the pattern camera and all other light to the white light camera. By adapting to standard laparoscopes and ensuring that all customized hardware is outside the patient's body, we simplify adoption of this technology into existing operating rooms.

structures in 3-dimensions [2]–[6]. However, the well-known stereo correspondence problem, in which a point in one camera is ambiguous when imaged by the corresponding camera when sufficient texture is lacking, limits its utility. To address this, several investigators have explored structured light methods in which one of the cameras in the stereo system is replaced with an active illumination device that projects a known coded pattern into the scene [7]–[10]. These methods require a long scanning procedure or require multiple images of different patterns of light to code the scene and are not conducive to real-time 3D reconstruction. Another previously described method injects a single dot laser pointer into the scene to triangulate individual 3D points one-at-a-time, which also cannot deliver real-time 3D information [11].

More recent work addresses the real-time issue by developing a custom laparoscope and using a monochromatic coded pattern that can be matched in a single image with a spatial neighborhood matching scheme [12]. In [13], structured light is used with a spectrally encoded fiber-based lighting probe to recover intraoperative 3D information. However, both of these methods suffer from the fact that the projected light patterns are delivered in the visible spectrum and are not removed, and thus delivering an image to the surgeon with a distracting pattern during the procedure. Another group of investigators designed an alternative 3D methodology by designing a time-of-flight sensor fixed onto the endoscope hardware [14]. This modulates a light source at a very high frequency and measures the depth of scene points using knowledge of the fixed speed-of-light, however, only  $\sim 3000$  points were reconstructed at 20Hz and no color information was provided in this reconstruction.

In this paper, we present our SSL system for intraoperative 3D imaging during MIS. Our system is unique for the following reasons:

- It is constructed using standard, off-the-shelf laparoscopes and cameras, simplifying adoption of this technology into current operating rooms.

- It has the potential to become a low cost add-on to existing stereo laparoscopes.
- We ensure that our pattern is invisible to the surgeon to reduce distractions during the procedure.
- We solve the lack of depth perception by building a 3D model by using a computational, rather than a perceptual, approach.
- Our User Interface follows a hybrid approach allowing 3D visualizations side-by-side with a standard color 2D images enabling the surgeon to obtain different views.
- Our device provides metrology, allowing us to precisely measure sizes of structures (e.g. tumors) and distances between structures.

Furthermore, we show preliminary results of the accuracy of our reconstruction system and discuss our work towards developing an intuitive user interface for interaction with this new type of live image information which can enable a more informative surgical experience.

## II. SYSTEM OVERVIEW

Structured Light (SL) is a well-known technique for recovering 3D information in which a known pattern of light is projected onto a scene and then imaged with a camera system. By analyzing how the pattern in the reflected light is distorted by the reflecting surface of the scene, the 3D nature of the surface of the site in that scene can be accurately reconstructed using computational techniques. We begin by describing the hardware design for our prototype SSL system, followed by the software and algorithms developed for 3D reconstruction of the scene. Finally, we present experimental results using the SSL system. Fig. 1 is an overview of the system and we describe it in more detail below.

### A. Hardware

Our prototype SSL system begins with two standard, off-the-shelf, side-by-side 10mm laparoscopes (Fig. 2), two Point Grey Firefly MV FMVU-13S2C [15] color cameras, and a narrow-band 460nm blue LED light projector coupled with

a custom-designed pattern dispersion photomask [16]. The photomask is attached to the end of the LED light projector and projected down one of the laparoscopes (the "projection channel"). The narrow-band light projector is chosen in a range of the visible spectrum that can safely be removed without the surgeon realizing a strong difference in the color of the images when presented with this narrow-band removed via optical filters. The photomask (Fig. 3, right) is designed as a De Bruijn sequence pattern of vertical lines [9]. Because we know the exact range of blue light contained within the pattern, we can attach a center-pass optical filter on a camera coincident with the second laparoscope (the "reception channel") so that the camera sees nothing but the blue pattern light for the purposes of structured light reconstruction. This simplifies the process of identifying the pattern in the surgical scene amongst all other light and structures that are present. We simultaneously deliver a standard white light source through a ring of optical fibers around the periphery of the "reception" laparoscope, exactly as all standard laparoscopes deliver white light to the surgical field. This white light also has the narrow-band blue wavelength removed to avoid confusion with the blue light being delivered by our pattern projector.

The reception channel receives all of the light in the scene, both the blue pattern light and all of the standard light of the surgical site. At the proximal side of the laparoscope (outside the patient's body), a dichroic beam splitter splits the outgoing light into two orthogonal directions. The dichroic beam splitter also filters the light so that in one direction, only the blue light which was delivered through the LED pattern projector is relayed, while the orthogonal direction receives all other light (minus the blue pattern light). Fig. 3 shows a plastic organ model (of a stomach) imaged on the left and the associated projected photomask pattern with the blue light on the right. In this way we have a "pattern camera" and an "imaging camera". Because the pattern camera only receives the blue pattern light, the detection and decoding of the pattern becomes less complicated than other structured light setups. Additionally, because we are only using blue light for this camera, we removed the Bayer pattern [17] (on the pattern camera only) so that every sensor unit receives unfiltered blue light. Finally, the imaging camera has the narrow-band blue pattern removed (by the dichroic beam splitter) and so the surgeon is not distracted by the blue De Bruijn sequence pattern during the procedure, and the 3D reconstruction becomes "invisible" to the surgeon.

## B. Software

Single-shot structured light [18] uses a single image as a template of the known pattern and matches subsequent images with 3D structure to the single image and decodes the warp of the pattern due to the 3D structure to recover the 3D information in the scene. We perform a procedure similar to the Microsoft Kinect, whereby an image of the De Bruijn sequence template is taken at a flat, parallel plane at a known distance from the tip of the laparoscope distal tips. The settings of the cameras are set to maximize the

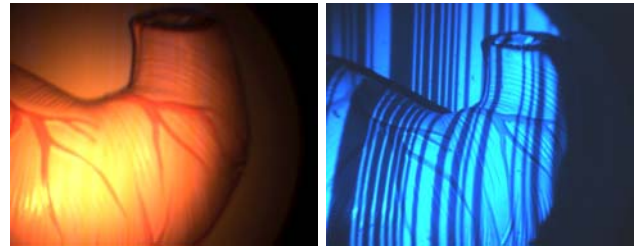


Fig. 3. **Left:** A plastic organ model of a stomach imaged using the white light imaging camera. Notice that none of the blue light from the LED pattern projector is present in this image, which is presented to the surgeon as the main 2D imaging source during a procedure. **Right:** The associated projected photomask pattern with the blue light on the same stomach model, used to reconstruct the object densely in 3D.

contrast of the edges in the vertical line De Bruijn sequence pattern. Then, for subsequent frames, we detect the warped De Bruijn sequence pattern and match, line-by-line, the correspondences to the template pattern on each scanline of the image separately. In this way, as the 3D structure of the scene warps the template, the horizontal disparity changes according to the amount of 3D structure compared to the flat image of the same template image.

To demonstrate the accuracy of the system, we label each image pair to identify all of the vertical lines in the image from the pattern. Next, we analyze each scanline, one-at-a-time, and match-up scanlines between the test and template images. As each "bar" in the template pattern begins, we automatically find the corresponding bar endpoint in the test image, assuming that horizontal scanlines correspond due to stereo epipolar undistortion [19]. In order to undistort the images from lens distortion, we pre-calibrate both the pattern and imaging camera using standard camera calibration techniques [20]. Also, because there are two cameras, we calibrate the pattern and imaging cameras to each other as a stereo camera rig to recover the stereo extrinsics as a rigid body rotation and translation, allowing us to lookup RGB color values for each 3D point recovered.

Because we can only correspond the edges of a bar in the pattern, we linearly interpolate the horizontal disparity in between every pair of lines representing a complete "bar" in the pattern. This assumption requires a smooth transition of depth within the confines of a single bar, and by using thin enough bars, this can be reasonably achieved. In the end, we compute a full horizontal disparity image between a test image and the template image.

1) *Depth From Disparity:* In a typical stereo setup, depth can be recovered from horizontal disparity using the following relationship:

$$z = \frac{b * f}{d} \quad (1)$$

In this equation,  $z$  is the depth (in meters),  $b$  is the calibrated horizontal baseline between the cameras (in meters),  $f$  is the (common) focal length of the cameras (in pixels), and  $d$  is the disparity (in pixels). Based on this relationship, as disparity approaches zero, the depth approaches infinity. However,

in our customized structured light setup, because we are capturing an image of our template at a known (positive) distance from the cameras, zero disparity now corresponds to this known distance rather than infinity, and Eq. 1 must be adjusted:

$$z = \frac{b * f}{d_{off} - d} \quad (2)$$

In this equation,  $d_{off}$  represents the disparity offset due to the distance to the known template image in order to re-normalize zero disparity to the correct depth. The value of  $d_{off}$  is computed empirically using a cylinder calibration object by mapping known depth values to known disparity values and recovering the best fit estimate of  $d_{off}$ . Once we have a depth value at every pixel (and the focal length ( $f_x$ ,  $f_y$ ) and principal point ( $c_x$ ,  $c_y$ ) of the pattern camera), we can recover a 3D point at every pixel as:

$$x = z * \frac{u - c_x}{f_x}, \quad y = z * \frac{v - c_y}{f_y} \quad (3)$$

where  $(u, v)$  is the pixel corresponding to the depth value  $z$ . In this way, given an arbitrary image, we:

- Compute line-by-line correspondences of the vertical lines in the De Bruijn sequence pattern from a test image to the template image
- Linearly-interpolate the horizontal disparity in-between every line pair correspondence
- Convert disparity to depth using Eqn. 2
- Recover the 3D point cloud using the depth image at every pixel using Eqn. 3

2) *Colorizing the Point Cloud*: Finally, because we wish to display a graphically-pleasing colored 3D point cloud, we use the stereo extrinsics between the pattern and imaging cameras to assign an RGB color to every 3D point recovered from the depth image. To do this, we first compute every 3D point with respect to the blue camera, as described in Sec. II-B.1. Next, we apply the rigid-body stereo extrinsics recovered from the camera calibration to represent this 3D point with respect to the imaging camera. Finally, we apply the imaging camera’s intrinsics to look-up the corresponding RGB color information for this 3D point, allowing us to render a photo-realistic 3D rendering of the scene on-the-fly.

3) *Developing a User Interface*: To enable the surgeon to visualize and perform online transformations on the 3D reconstructed images during an in-vivo procedure, we developed an early prototype user interface.

Using our prototype SSL Thumbstick (Fig. 4), an add-on 2-axis button joystick mounted on standard laparoscopic tools, the surgeon is able to operate in three different modes: 1) Standard live 2D image mode, 2) Side-by-side mode of the live 2D image and the 3D reconstructed view (Fig. 5), and 3) 3D reconstructed view mode (Fig. 6).

In Fig. 5 we show the side-by-side mode of a cylinder where the surgeon can see both the live 2D image from the online in-vivo procedure and the 3D reconstructed view, allowing her/him to manipulate the 3D display, for example,



Fig. 4. An image of our prototype SSL Thumbstick. We use a 2-axis button joystick as an add-on to a standard, off-the-self laparoscopic tool to allow the surgeon to perform virtual transformations (translate, rotate and scale) to 3D reconstructed images or Zoom and Pan 2D Images without having to take her/his hands of the laparoscopic tools or change the position of the laparoscopic camera.

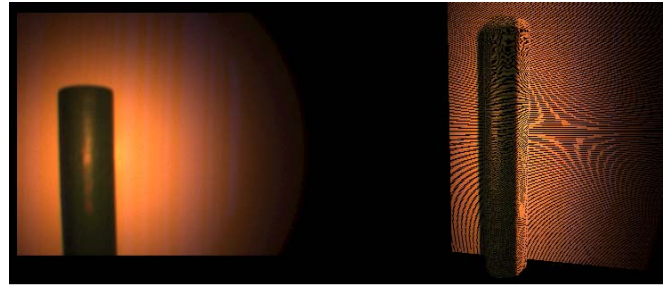


Fig. 5. Screen capture of our user interface. **Left**: Picture of a 2D Image of the cylinder object. **Right**: The 3D reconstructed model of the same cylinder using the SSL system. Here, we aim to display both the 2D and 3D image information to the surgeon in a useable and intuitive fashion. Because we are providing colorized 3D point cloud information, the surgeon is able to move, rotate and zoom (virtually) on our reconstructed 3D model to view the anatomy from various viewpoints, a capability which is not possible with current intra-operative imaging techniques.

to zoom in on an organ or rotate the viewpoint while maintaining full view and locus with the 2D image on the other side.

In Fig. 6 we show the 3D reconstruction view mode of a cylinder and a plastic organ (Heart). Since a 3D model has been reconstructed, the surgeon can rotate and translate the model to obtain novel views of the anatomy that are not possible with a standard 2D image.

The approach suggested is unobtrusive to the surgeon and from a User Interface perspective, complies with Schneiderman’s Visual Information-Seeking Mantra [21], providing the surgeon the amount of information s/he needs exactly when s/he needs it. In addition to that, the surgeon is not required to take her/his hands off the laparoscopic tools at any time or move back and forth the actual laparoscopic camera to obtain a different view. Such capabilities are not possible with current intra-operative imaging techniques.

### III. EXPERIMENTS & RESULTS

We demonstrate the accuracy of our SSL system using ex-vivo data on both a cylinder calibration object (Fig. 7, top-row) as well as various plastic organs (Fig. 7, rows 2-4). Although we are not explicitly dealing with in-vivo environments yet, these experiments show the potential of

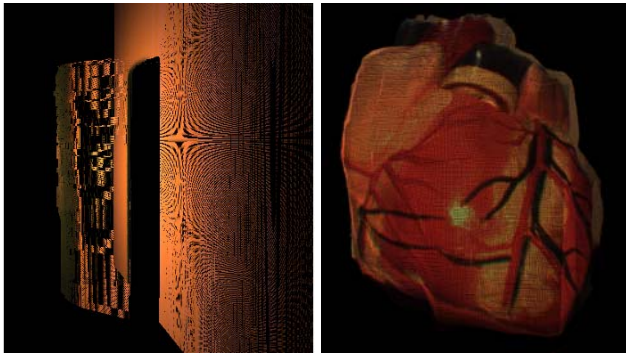


Fig. 6. **Left:** Screen capture of our user interface. Here, we aim to show an additional Side View of the colorized 3D point cloud information of the cylinder portrayed on Fig. 5. Using the SSL thumbstick (Fig. 4), the surgeon is able to move, rotate and zoom (virtually) on our reconstructed 3D model without the need to reposition the laparoscopic camera or take her/his hands of the laparoscopic tools. **Right:** Another screen capture of our 3D viewer from our user interface showing a heart model reconstruction from a different viewpoint, further displaying our capabilities of novel viewpoints which are different from the 2D color camera's (fixed) viewpoint.

our 3D sensor system. In order to reconstruct any object, we first must capture a *template* image, showing an unobstructed view of our De Bruijn sequence pattern on a flat parallel plane. An example of this is shown in Fig. 3, right. Additionally, we must estimate the  $d_{off}$  parameter described in Eqn. 2 which maps zero-disparity values to a known positive depth distance. We do this empirically using our cylinder object to estimate  $d_{off}$  by corresponding disparity values to known depth values.

Next, we capture an image of our calibration cylinder, with a pre-measured diameter of 17.50mm. The first row of Fig. 7 shows the white light and blue pattern images in the first and second columns, respectively. We then match the pattern lines in the cylinder's blue pattern image to our template pattern image, recovering the horizontal pixel disparity at every pixel in the image, and then recover the depth image using Eqn. 2 as shown in the third column. Finally, using Eqn. 3 we reconstruct the cylinder object in 3D and assign an RGB color to each 3D point using the technique described in Sec. II-B.2, producing a dense, photo-realistic 3D reconstruction of the cylinder in the fourth column of Fig. 7. To measure the accuracy, we calculated the diameter of our cylinder reconstruction, resulting in an error of 0.20mm. Furthermore, we analyzed the distance from the tip of the laparoscope to a flat plane at a known distance immediately anterior to the object, positioned at exactly 100.00 mm (measured with calipers) along the optical axis. Our reconstruction showed an error of 0.30mm to this flat plane. We note that typical errors in stereo reconstruction fall mostly along the optical z-axis of camera systems, and so our sub-millimeter error rate along this axis direction is very encouraging.

To further test our system, we performed reconstructions on 2 plastic organs, shown in Fig. 7 on rows 2 (Heart), and 3 (Brain Segment). For each example, the first column shows the white light image, noting that the blue pattern is completely removed through our dichroic beam splitter

so that the surgeon's view is unobstructed by the De Bruijn sequence pattern. The second column for each shows the blue pattern camera with the object that we wish to reconstruct. The third column shows the resulting depth image after matching the pattern in the blue camera to our pre-captured template image, and finally a colored, photo-realistic 3D reconstruction in the fourth column.

One advantage of our SSL system is that we are able to assign accurate color information to each 3D point in the reconstruction. We are able to achieve this solely due to the fact that the white light color image has the pattern removed, whereas in other implementations of MIS structured light the projected light source would show up in the reconstruction, and so no color information can be provided. This allows the surgeon to approach the object (virtually) from different angles and viewpoints through our user interface, and the color allows them to make sense of the information much easier than an uncolored reconstruction might.

#### IV. CONCLUSIONS & FUTURE WORK

In this paper we have presented a novel 3D imaging device that provides an accurate 3D model of internal anatomy using a standard laparoscope system. The hardware is constructed from standard, off-the-shelf cameras and laparoscopes that can be easily adopted into current ORs. We have also presented an initial user interface for the system that will allow the surgeon to control both 2D and 3D images online during a procedure.

Our current prototype uses two side-by-side laparoscopes, one for projection and one for reception. We hope to port this system to a stereo laparoscope which will reduce the size and allow for standard minimally invasive surgery, and motivate using the system as an add-on to existing stereo laparoscopes.

We are currently speeding up the organ reconstruction method to make it a real-time process. This will allow the surgeon to view the 3D information at the same frame rate as the standard 2D laparoscopic image. The blue light camera is currently providing images at 1Hz due to light attenuation, however there are faster and more sensitive cameras which we are currently investigating, which can provide a higher update rate. Another improvement is to change the photomask to provide higher resolution and more accurate results. We are also beginning initial trials of an improved user interface using the SSL thumbstick interface with clinical fellows.

An important side effect of generating an accurate 3D model is the ability to do metrology on the organ model. This will allow the surgeon to take online measurements in-vivo during a procedure that will assist her or him. This creates a virtual ruler and eliminates the need to insert a physical ruler into the body. Also the ability to manipulate the generated model to provide novel views while still viewing the 2D image may prove important to the surgeon. Finally, with an accurate 3D model, we have the capability to register preoperative images with online in-vivo anatomy.

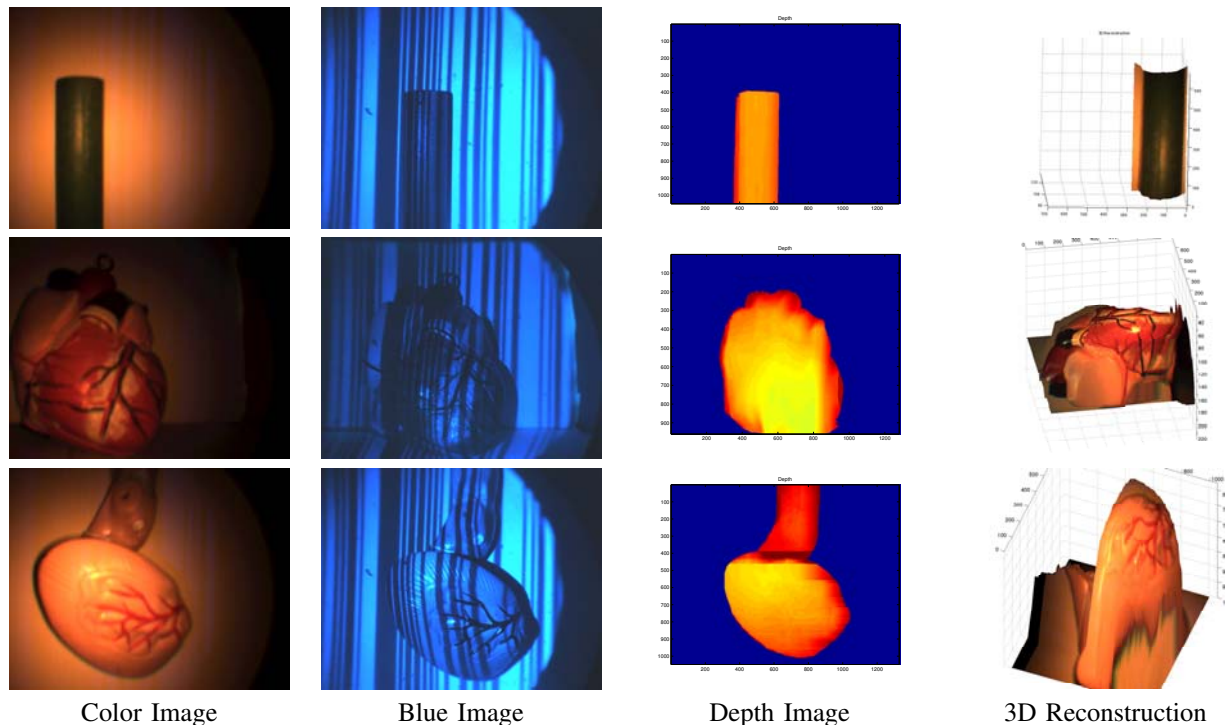


Fig. 7. Experimental results of our SSL prototype system. **First Column:** The white light images of each experiment. **Second Column:** The associated blue pattern image used for the 3D reconstruction. **Third Column:** The resulting depth images after corresponding the pattern images with the template image. **Fourth Column:** The colored photo-realistic 3D reconstructions. **Top Row:** Results of our calibration cylinder, to gauge numerical accuracy of our SSL system. **Second and Third Row:** Results on plastic organs of a heart and a brain segment, respectively. In each example, the 3D structure of the objects are accurately captured and we are able to then rotate and zoom-in on the reconstructions intra-operatively.

## REFERENCES

- [1] L. Way, K. Stewart, W. Gantert, K. Liu, C. Lee, and e. a. Whang, K., "An analysis of 252 cases from a human factors and cognitive psychology perspective," *Annals of Surgery*, vol. 237, pp. 460–469, 2003.
- [2] L. Maier-Hein, P. Mountney, A. Bartoli, H. Elhawary, D. Elson, A. Groch, A. Kolb, M. Rodrigues, J. Sorger, S. Speidel, et al., "Optical techniques for 3d surface reconstruction in computer-assisted laparoscopic surgery," *Medical Image Analysis*, 2013.
- [3] M. Hu, G. Penney, P. Edwards, M. Figl, and D. J. Hawkes, "3d reconstruction of internal organ surfaces for minimal invasive surgery," in *Medical Image Computing and Computer-Assisted Intervention—MICCAI 2007*. Springer, 2007, pp. 68–77.
- [4] W. W. Lau, N. A. Ramey, J. J. Corso, N. V. Thakor, and G. D. Hager, "Stereo-based endoscopic tracking of cardiac surface deformation," in *Medical Image Computing and Computer-Assisted Intervention—MICCAI 2004*. Springer, 2004, pp. 494–501.
- [5] D. Stoyanov, A. Darzi, and G. Z. Yang, "Dense 3d depth recovery for soft tissue deformation during robotically assisted laparoscopic surgery," in *Medical Image Computing and Computer-Assisted Intervention—MICCAI 2004*. Springer, 2004, pp. 41–48.
- [6] H. Haneishi, T. Ogura, and Y. Miyake, "Profilometry of a gastrointestinal surface by an endoscope with laser beam projection," *Optics letters*, vol. 19, no. 9, pp. 601–603, 1994.
- [7] C. Schmalz, F. Forster, A. Schick, and E. Angelopoulou, "An endoscopic 3d scanner based on structured light," *Medical Image Analysis*, vol. 16, no. 5, pp. 1063–1072, 2012.
- [8] M. Hayashibe, N. Suzuki, and Y. Nakamura, "Laser-scan endoscope system for intraoperative geometry acquisition and surgical robot safety management," *Medical Image Analysis*, vol. 10, no. 4, pp. 509–519, 2006.
- [9] J. Salvi, J. Pages, and J. Batlle, "Pattern codification strategies in structured light systems," *Pattern Recognition*, vol. 37, no. 4, pp. 827–849, 2004.
- [10] J. D. Ackerman, K. Keller, and H. Fuchs, "Surface reconstruction of abdominal organs using laparoscopic structured light for augmented reality," in *Electronic Imaging 2002*. International Society for Optics and Photonics, 2002, pp. 39–46.
- [11] M. Hayashibe and Y. Nakamura, "Laser-pointing endoscope system for intra-operative 3d geometric registration," in *IEEE Intl. Conf. on Robotics and Automation*, 2001.
- [12] X. Maurice, C. Albitar, C. Doignon, and M. de Mathelin, "A structured light-based laparoscope with real-time organs' surface reconstruction for minimally invasive surgery," in *Engineering in Medicine and Biology Society (EMBC), 2012 Annual International Conference of the IEEE*. IEEE, 2012, pp. 5769–5772.
- [13] N. Clancy, D. Stoyanov, L. Maier-Hein, A. Groch, G. Yang, and D. Elson, "Spectrally encoded fiber-based structured lighting probe for intraoperative 3d imaging," *Biomedical Optics Express*, vol. 2, no. 11, pp. 3119–3128, Nov 2011.
- [14] J. Penne, K. Höller, M. Stürmer, T. Schrauder, A. Schneider, R. Engelbrecht, H. Feußner, B. Schmauss, and J. Hornegger, "Time-of-flight 3-d endoscopy," in *Medical Image Computing and Computer-Assisted Intervention—MICCAI 2009*. Springer, 2009, pp. 467–474.
- [15] P. G. R. Inc. (2013) Firefly mv cameras. [Online]. Available: <http://www.ptgrey.com>
- [16] K. Konolige, "Projected texture stereo," in *Robotics and Automation (ICRA), 2010 IEEE International Conference on*, 2010, pp. 148–155.
- [17] B. E. Bayer, "Color imaging array," *US Patent*, vol. US3971065 A, 07 1976.
- [18] C. Schmalz and E. Angelopoulou, "Robust single-shot structured light," in *IEEE Intl. Workshop on Projector-Camera Systems*, 2010.
- [19] R. Hartley and A. Zisserman, *Multiple View Geometry in Computer Vision*, 2nd ed. New York, NY, USA: Cambridge University Press, 2003.
- [20] Z. Zhang, "A flexible new technique for camera calibration," *IEEE Transactions on Pattern Analysis and Machine Intelligence*, vol. 22, no. 11, pp. 1330–1334, 2000.
- [21] B. Shneiderman, "The eyes have it: A task by data type taxonomy for information visualizations," in *Visual Languages, 1996. Proceedings., IEEE Symposium on*. IEEE, 1996, pp. 336–343.